Development 140, 1796-1806 (2013) doi:10.1242/dev.091157

Notch and Nodal control forkhead factor expression in the specification of multipotent progenitors in sea urchin

Stefan C. Materna[1,*,‡], S. Zachary Swartz[2] and Joel Smith[1,2,3,‡]

SUMMARY

Indirect development, in which embryogenesis gives rise to a larval form, requires that some cells retain developmental potency until they contribute to the different tissues in the adult, including the germ line, in a later, post-embryonic phase. In sea urchins, the coelomic pouches are the major contributor to the adult, but how coelomic pouch cells (CPCs) are specified during embryogenesis is unknown. Here we identify the key signaling inputs into the CPC specification network and show that the forkhead factor *foxY* is the first transcription factor specifically expressed in CPC progenitors. Through dissection of its cis-regulatory apparatus we determine that the *foxY* expression pattern is the result of two signaling inputs: first, Delta/Notch signaling activates *foxY* in CPC progenitors; second, Nodal signaling restricts its expression to the left side, where the adult rudiment will form, through direct repression by the Nodal target *pitx2*. A third signal, Hedgehog, is required for coelomic pouch morphogenesis and institution of laterality, but does not directly affect *foxY* transcription. Knockdown of *foxY* results in a failure to form coelomic pouches and disrupts the expression of virtually all transcription factors known to be expressed in this cell type. Our experiments place *foxY* at the top of the regulatory hierarchy underlying the specification of a cell type that maintains developmental potency.

KEY WORDS: FoxY, Hedgehog, Notch, Coelomic pouch, Left/right asymmetry, Multipotency, *Strongylocentrotus purpuratus*

INTRODUCTION

The ability of certain cells to resist differentiation is an important feature of animal development. Most notably, sexually reproducing animals establish germ line stem cells that create the sperm and eggs required for fertilization (Spradling et al., 2011). In animals undergoing indirect development, embryogenesis results in a larval form that may differ dramatically from the adult organism (Minelli, 2009). This requires that some cells are either segregated away during embryogenesis and remain multipotential, or that they reacquire multipotency, in order to contribute to the diverse tissues of the adult, including the germ line (Arenas-Mena, 2010).

In sea urchins, embryogenesis gives rise to a feeding larva, which after a prolonged period of time will produce the adult. A prerequisite for rudiment formation is the specification of coelomic mesoderm, a group of cells derived from the veg2 lineage that gives rise to two pouch-like protrusions at the tip of the archenteron (Cameron et al., 1991). Rudiment formation commences with the invagination of a piece of ectodermal wall above the left coelomic pouch. A complex morphogenetic process ensues, during which the adult body plan with its pentameral symmetry is established (Pearse and Cameron, 1991). In *Strongylocentrotus purpuratus*, each of the coelomic pouches initially contains only about ten cells, but their descendants are major contributors to various adult structures (Pearse and Cameron, 1991); at metamorphosis, ~90% of the 150,000 larval cells are located in the juvenile (Cameron et al., 1989; Song and Wessel, 2012), illustrating that coelomic pouch cells are multipotent progenitors.

[1]California Institute of Technology, Division of Biology, m/c 156-29, Pasadena, CA 91125, USA. [2]Brown University, Department of Molecular Biology, Cell Biology and Biochemistry, 185 Meeting Street, Providence, RI 02912, USA. [3]Marine Biological Laboratory, 7 MBL Street, Woods Hole, MA 02543, USA.

*Present address: Cardiovascular Research Institute, UCSF, 555 Mission Bay Blvd South, MC 3120, San Francisco, CA 94158, USA
‡Authors for correspondence (stefan.materna@ucsf.edu; jcsmith@mbl.edu)

Accepted 18 February 2013

In euechinoid sea urchins, coelomic pouch cell (CPC) progenitors are specified during gastrulation as a consequence of Delta/Notch (D/N) signaling within the non-skeletogenic mesoderm (NSM) (Sherwood and McClay, 1999; Sweet et al., 2002). Interference with NSM Delta abolishes coelomic pouch formation but does not disrupt the specification of other mesodermal cell types specified earlier (Materna and Davidson, 2012; Materna et al., 2013; Sweet et al., 2002). During archenteron formation, the CPC progenitors are located at the tip but then split into two groups that relocate laterally to either side of the foregut. Although little is known about the regulation of this morphogenetic process, the expression of Hedgehog (Hh) in the adjoining endoderm and of its receptors in CPC progenitors (Walton et al., 2009) suggests the possible involvement of this signal. The small micromeres (SMMs) are also located at the tip of the archenteron and are distributed to either coelomic pouch at the pluteus stage (Pehrson and Cohen, 1986). They are set aside and remain mitotically quiescent during embryogenesis (Tanaka and Dan, 1990). The SMMs express orthologs of numerous germ line/stem cell markers (Juliano et al., 2010; Voronina et al., 2008) and are required to form the germ line in *Lytechinus variegatus* (Yajima and Wessel, 2011), and thus might be primordial germ cells. However, whether they also contribute to other tissues remains unresolved.

The forkhead factor *foxY*, originally named *foxC* (Ransick et al., 2002; Tu et al., 2006), is the first transcription factor to be specifically expressed in any of the cells that contribute to the coelomic pouches. At early blastula stage, *foxY* is expressed in the SMMs in response to D/N signaling originating in the skeletogenic lineage (Materna and Davidson, 2012), then at the tip of the archenteron and in both coelomic pouches as they form. At late gastrula stage, *foxY* becomes strongly biased to the left coelomic pouch, presumably as a consequence of Nodal signaling establishing left/right (L/R) asymmetry across the embryo (Duboc et al., 2005). Although many transcription factors are eventually expressed in the coelomic pouches (Duboc et al., 2005; Howard-Ashby et al., 2006a; Howard-Ashby et al., 2006b; Luo and Su,

2012; Poustka et al., 2007; Tu et al., 2006), when CPC progenitors are first specified *foxY* is the only gene to become expressed in direct response to NSM Delta among 182 known regulatory genes, most of them with spatially restricted expression (Materna and Davidson, 2012; Ransick et al., 2002; Tu et al., 2006). This suggests that *foxY* plays an important role in coelomic pouch formation.

Here we examine the regulation and significance of *foxY* expression and find that it is essential for the specification of CPCs. Its precise expression pattern is the result of the integration of the D/N and Nodal signals within the *foxY* regulatory region: D/N signaling directly activates *foxY* expression, first in SMMs and then in CPC progenitors, while Nodal represses *foxY* in the right coelomic pouch via Pitx2. Reception of the Hh signal in CPC progenitors sets in motion coelomic pouch morphogenesis, but does not directly affect *foxY* expression. However, Hh is required for proper Nodal expression on the right side of the embryo and is thus involved in the establishment of L/R asymmetry. Our results link *foxY* directly to the specification of a cell type with great developmental potency en route to formation of the adult.

MATERIALS AND METHODS

Perturbation experiments

FoxY morpholino antisense oligonucleotide (MASO) (5′-CATGGCTC-CAAGTGCAGAACACTAC-3′) was obtained from Gene Tools (Pilomath, OR, USA) and injected at 300 μM in 0.12 M KCl. A random MASO (N_{25}) was injected as a control; injection volumes were 5 pl. DAPT and SB431542 were applied as reported previously (Materna and Davidson, 2012; Materna et al., 2013). Cyclopamine was dissolved in ethanol and added to a final concentration of 0.5 μM. A corresponding volume of solvent was added to controls.

RNA extraction and transcriptional profiling

Sea urchin (*Strongylocentrotus purpuratus*) embryos were cultured at 15°C. RNA was extracted using the RNeasy Micro Kit (Qiagen, Hilden, Germany) according to the manufacturer's instructions. Expression levels were quantified with the NanoString nCounter (NanoString, Seattle, WA, USA) using a probe set for 205 genes. Samples were processed according to the manufacturer's instructions and data processed as described (Materna and Davidson, 2012). Data were supplemented by quantitative PCR (QPCR) for *nanos* and fold changes calculated using *poly-ubiquitin* and *hmg1* as references (Materna and Oliveri, 2008). A threshold of 2-fold difference was chosen as a significant change (Materna and Oliveri, 2008). QPCR primer sequences are included in supplementary material Table S1. Code set information and all perturbation data are available at the Dryad Digital Repository (http://dx.doi.org/10.5061/dryad.np321).

Whole-mount *in situ* hybridization (WMISH)

WMISH was conducted following standard procedures (Materna and Davidson, 2012). In brief, templates were amplified by PCR (for primers, see supplementary material Table S1) and used for transcription of digoxigenin (DIG)-labeled probes. Embryos were fixed in 2.5% glutaraldehyde, 32.5% sea water, 32.5 mM MOPS (pH 7) and 162.5 mM NaCl on ice overnight. Embryos were proteinase K treated for 5 minutes at room temperature [25 ng/μl in TBST (0.1 M Tris pH 7.5, 0.15 M NaCl, 1% Tween 20)] followed by 30-minute fixation in 4% paraformaldehyde, 32.5% sea water, 32.5 mM MOPS (pH 7), 162.5 mM NaCl at room temperature. Probes were hybridized overnight and detected using anti-DIG Fab fragments conjugated to alkaline phosphatase (Roche). Color was developed using NBT/BCIP reagents (Roche); fluorescent *in situ* hybridizations were developed using TSA amplification (PerkinElmer).

Immunofluorescence

In situ stained embryos were colabeled by immunofluorescence for Vasa protein. Following a 30-minute blocking step (TBST, 10% sheep serum), embryos were incubated overnight with Vasa antibody (Voronina et al., 2008) diluted 1:250 in TBST with serum. Embryos were washed three times for 15 minutes each with TBST without serum, and incubated for 2 hours with Cy3 goat anti-rabbit secondary antibody (Invitrogen) diluted 1:250 in TBST with serum. Embryos were then washed three times in TBST buffer and imaged.

Phalloidin staining

F-actin was visualized by Rhodamine phalloidin staining (Strickland et al., 2004). In brief, embryos were fixed for 1 hour in Millonig's phosphate-buffered fixative followed by two washes in 50 mM HEPES, 50 mM PIPES, 0.6 M mannitol, 3 mM $MgCl_2$, 0.1% Triton X-100, pH 7.0. Embryos were transferred to TBST and stained with Rhodamine phalloidin in TBST (2 U/ml) for 1 hour. Embryos were washed three times and then imaged.

Reporter assays

About 1500 molecules of reporter construct in ~4 pl were co-injected with a 6-fold molar excess of carrier DNA in 0.12 M KCl. BAC reporters were constructed as reported previously (Smith, 2008) and injected with 400 copies of BAC per 4 pl without carrier. Spatial activity was assessed by fluorescence microscopy. All experiments were repeated in different batches of eggs. Cis-regulatory regions were identified as described (Smith, 2008). For target site disruptions, C bases were mutated to T, and A bases were mutated to G, and vice versa, for invariant bases in consensus sites. 5′-(C/T)(A/G)TG(A/G)GA(A/G/T)-3′ was used to identify candidate Su(H) sites (Ransick and Davidson, 2006). The TG at positions 3/4 and the GA at positions 6/7 were mutated to CA and AG, respectively. 5′-GGATTA-3′ was used to identify candidate Pitx2 target sites, and 5′-GATT-3′ was mutated to 5′-AGCC-3′.

RESULTS

foxY expression in sea urchin embryogenesis

At early blastula stage, *foxY* is expressed in the SMMs at the vegetal pole of the embryo. During gastrulation it is expressed at the tip of the archenteron, but eventually becomes restricted to the left coelomic pouch (Ransick et al., 2002). As has been suggested by a recent study (Song and Wessel, 2012), the *foxY* expression domain might not be restricted to the SMMs during gastrulation, but instead may expand to include the NSM. We set out to obtain a better understanding of *foxY* expression.

A time series of *foxY* gene expression (Materna et al., 2010) revealed a biphasic profile through late gastrulation (Fig. 1A). The early expression phase lasts from ~9 hours postfertilization (hpf) until 23 hpf, i.e. from when the SMMs are born to the mesenchyme blastula stage. After a quick initial rise, *foxY* levels remain constant at ~140 transcripts per embryo (~35 copies in each SMM). Staining of *foxY* message overlaps with that of Vasa protein, an RNA helicase involved in translational control in primordial germ cells (Fig. 1B,C) (Gustafson and Wessel, 2010). Vasa is specific to SMMs (Gustafson and Wessel, 2010; Voronina et al., 2008), confirming that *foxY* expression is restricted to this cell type. The four SMMs are located at the vegetal pole and are in direct contact with the cells of the skeletogenic lineage. When the skeletogenic cells ingress into the blastocoel, the SMMs stay behind and come into contact with the NSM cells, which replace the skeletogenic cells in the vegetal plate (Fig. 1B,C).

During its second expression phase, *foxY* transcript levels increase significantly and reach a peak of ~500 transcripts/embryo at 30 hpf (Fig. 1A), followed by a steady decline. The rise of *foxY* transcript levels coincides with an expansion of the *foxY* expression domain (Fig. 1D-F); at 30 hpf *foxY* is expressed in the mesodermal cells, i.e. the veg2-derived CPC progenitors that directly surround the Vasa-positive SMMs (Fig. 1D). *foxY* is expressed throughout the cap of the elongated archenteron, whereas the SMMs remain located at the center (they have divided once; there are now eight Vasa-positive cells). Towards the end of gastrulation the cap bulges laterally to form the coelomic pouches, and *foxY* expression

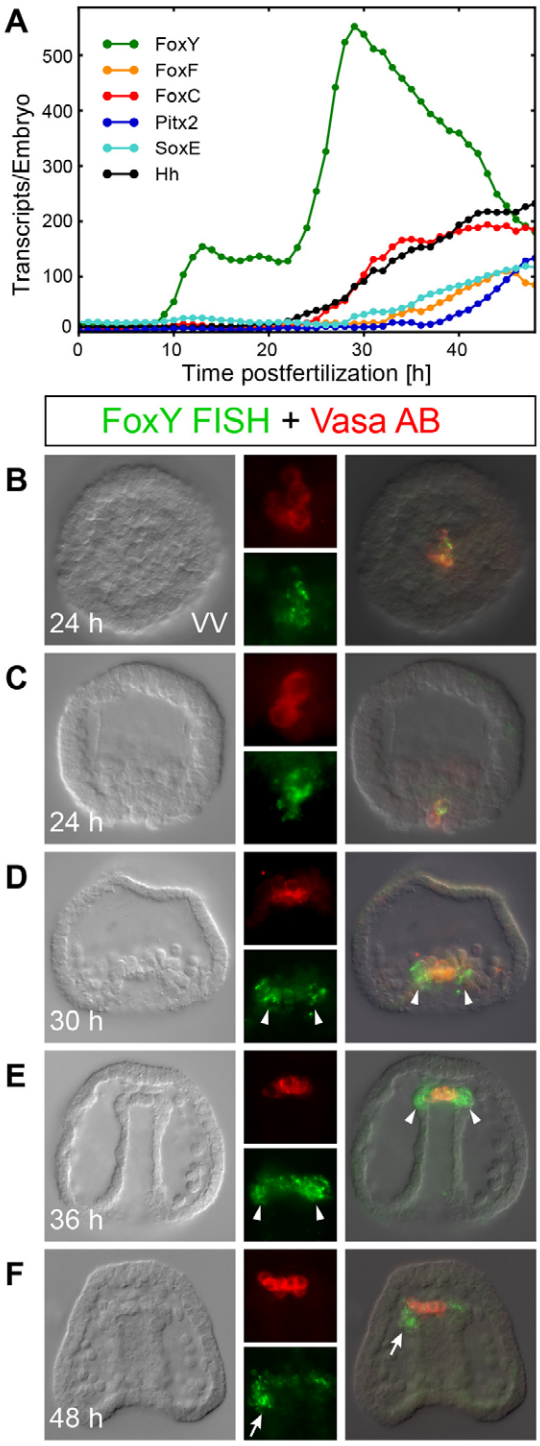

Fig. 1. Expression profiles of coelomic pouch cell (CPC) genes. (**A**) Temporal expression of sea urchin CPC genes from fertilization to late gastrulation. Levels are given in transcripts per embryo. (**B-F**) *foxY* mRNA (FISH)/Vasa protein (AB) staining. Left , differential interference contrast (DIC); center, *foxY* signal (green) and Vasa signal (red); right, merge. The magnified central panels capture all fluorescence. (B,C) Initially, *foxY* message is restricted to small micromeres (SMMs) and overlaps perfectly with Vasa. (D) *foxY* expression expands into mesodermal cells during gastrulation (arrowheads); SMMs are located at the archenteron tip. (E) By mid-gastrulation the entire archenteron tip expresses *foxY* (arrowheads). (F) *foxY* expression is biased toward the left coelomic pouch by 48 hpf (arrow). Lateral views, except vegetal view (VV) in B.

becomes strongly biased to the left coelomic pouch (Fig. 1E). SMMs are still located at the center of the archenteron tip (Fig. 1F), but staining for *foxY* message in the SMMs becomes progressively weaker and is barely visible at 48 hpf (Fig. 1F). This might indicate that the expression of *foxY* is not maintained in these cells, in agreement with the diminished number of *foxY*-positive cells (six to eight) at the early larval stage observed by Ransick et al. (Ransick et al., 2002). After ~3 days postfertilization (dpf), *foxY* is restricted to the left pouch (Ransick et al., 2002).

NSM Delta signaling specifies CPC progenitors

D/N signaling is active on three occasions during sea urchin embryogenesis: Delta is expressed in skeletogenic cells starting at ~9 hpf, then in NSM once skeletogenic cells have ingressed; it is also expressed in the apical plate, although its function here has not been studied in detail (Materna and Davidson, 2012; Smith and Davidson, 2008; Sweet et al., 2002; Walton et al., 2006). Delta expression in skeletogenic cells activates gene expression in the NSM and SMMs, which are both in direct contact with the Delta source. Importantly, *foxY* is the only known target that is specifically activated in the SMMs (Materna and Davidson, 2012). Disruption of the second, i.e. NSM, phase of D/N signaling with the Notch inhibitor DAPT prevents formation of the coelomic pouches. Among 182 known regulatory genes, the only one to be severely depleted at 30 hpf was *foxY* (Materna and Davidson, 2012) (supplementary material Fig. S1). As we have shown above, the strong increase in transcript levels between 23 and 30 hpf is due to activation of *foxY* in the mesodermal cells directly adjacent to the SMMs constituting the CPC progenitor population. The likely cause for this expansion is activation of *foxY* by D/N signaling originating in the NSM.

The timecourse data in Fig. 1A reveal that other genes restricted to CPCs (*foxF*, *pitx2*, *soxE*) are transcribed only at 30 hpf or thereafter. To better understand the role of D/N signaling in the specification of CPCs we extended the analysis of NSM Delta function into gastrulation. We added DAPT at 17 hpf, just prior to the activation of Delta in NSM, and quantified the perturbation effects on transcript levels with the NanoString nCounter (Geiss et al., 2008). We made use of a code set containing probes for all relevant transcription factors known to be expressed in a spatially restricted fashion, plus probes for several signaling ligands and marker genes. Probe sequences and accession numbers for all 205 genes included in our code set are available from the Dryad Digital Repository (see Materials and methods).

Fig. 2A displays the quantitative perturbation data collected for a selection of genes. A table with perturbation data for all genes is available from the Dryad Digital Repository (see Materials and methods). As expected from the failure to form coelomic pouches, all genes specific to, and uniquely expressed in, CPCs were strongly depleted in perturbed embryos compared with controls. At mid-gastrula (38 hpf) this included the forkhead factors *foxC*, *foxF* and *foxY* (Tu et al., 2006), the Sox/HMG factor *soxE* (Duboc et al., 2005; Howard-Ashby et al., 2006a) and the zinc-finger gene *scratchX* (Materna et al., 2006). *gataE* and *pax6* are expressed in CPCs, but are also expressed in the gut and ectoderm (Fig. 3E,F; supplementary material Fig. S2B-C″). Independent expression in these compartments obscures the perturbation effects in our quantitative analysis. The spatial expression pattern of *scratchX* was unknown, but it is first expressed in CPC progenitors at the tip of the archenteron and later in both coelomic pouches (Fig. 3G; Fig. 5E). These perturbation effects remain strong until late gastrulation (48 hpf) with the exception of *foxY*, which is no longer significantly

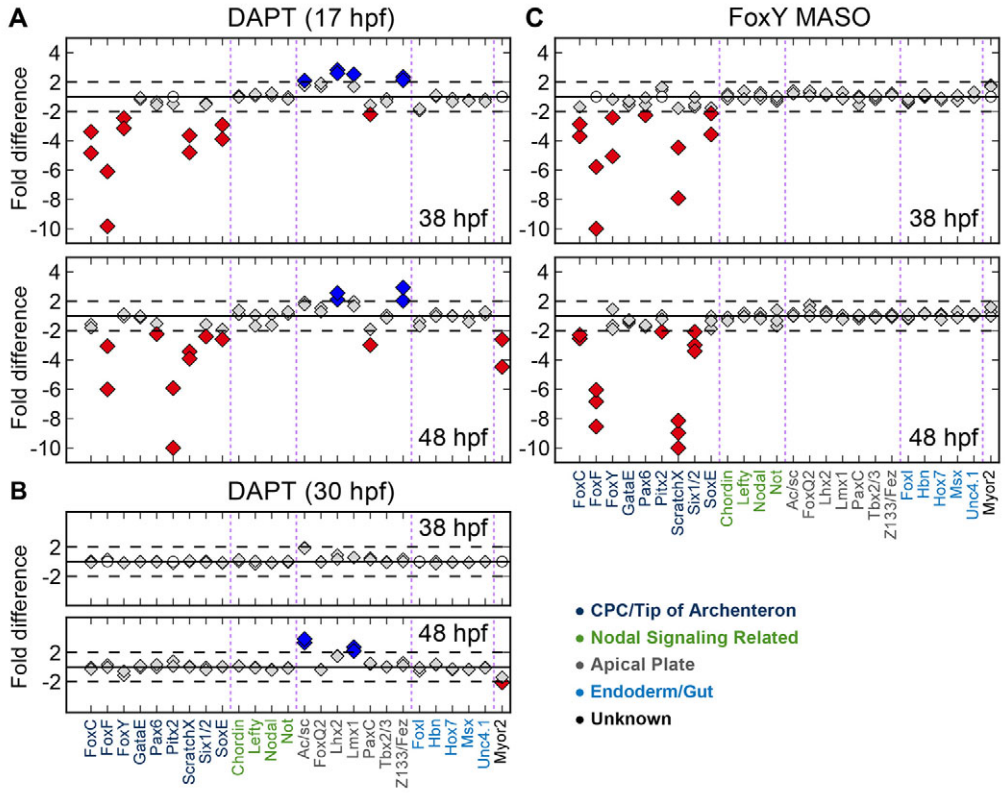

Fig. 2. Effects of Delta/Notch and FoxY perturbations on transcript levels for select genes. (**A**) Treatment with the Notch inhibitor DAPT at 17 hpf causes strongly reduced transcript levels of CPC genes and significantly affects the abundance of apical plate genes. (**B**) DAPT treatment at 30 hpf affects apical plate genes but not CPC genes. (**C**) Injection of FoxY morpholino antisense oligonucleotide (MASO) causes strong depletion of CPC genes only. Each diamond represent a single experiment; red indicates a significant reduction, blue an increase, and gray no significant change in transcript levels following treatment. Genes not significantly transcribed in experiment and control are marked with an open circle. We estimated transcript levels by comparing our data with prior absolute measurements (Materna et al., 2010). A level of ~25 transcripts/embryo was chosen as indicating significant expression. Black dashed lines indicate threshold for significant changes following perturbation.

affected, nor highly expressed at this time (Fig. 1A). The homeobox gene *pitx2* and the bHLH gene *myor2*, which have become activated by 48 hpf, are also depleted. *pitx2* is expressed in CPCs, but strongly biased to the right (Duboc et al., 2005; Luo and Su, 2012). The expression level of *myor2* is extremely low and we were unable to determine its spatial expression pattern. Endoderm genes are not activated by NSM Delta throughout gastrulation (Fig. 2A) (Materna and Davidson, 2012), despite strong expression of the Notch receptor in the archenteron (Walton et al., 2006).

To better understand the timing of the D/N signaling input into CPCs, we attempted to determine the spatial expression of *delta* during gastrulation. Similar to results reported by Walton et al. (Walton et al., 2006), we observed *delta* expression in dispersed cells in the ectoderm and in the apical plate (not shown), where it is an ongoing input into neurogenic genes (Fig. 2A). But owing to its low abundance (150 transcripts/embryo at 48 hpf) (Materna et al., 2010) and complex expression pattern we cannot rule out the possibility that low-level expression persists in single cells at the archenteron tip. To assess whether active Notch signaling is required for maintenance of CPC gene expression, we added DAPT at 30 hpf and quantified transcript levels. Our results show that some apical genes are strongly elevated at 38 and 48 hpf, indicating that D/N signaling is active in this domain. By contrast, no CPC gene is affected (Fig. 2B). These data suggest that the mesodermal Delta signal does not function as a continuous input into CPC genes during gastrulation. However, most CPC genes are activated after 30 hpf; in fact, *foxY* and *foxC* are the only known genes expressed in this compartment at 30 hpf (Fig. 1A). Thus, our findings imply that Delta activation of most CPC genes is indirect.

FoxY function is essential for coelomic pouch formation

foxY is the first known transcription factor to be specifically expressed in CPC progenitors downstream of Notch signaling. To test whether it is a potential regulator of other CPC genes we knocked down *foxY* expression with a MASO. FoxY MASO injection has no adverse effect on the health of the embryo and does not interfere with the general progression of development. The overall anatomy of the larvae is normal, including the skeleton and partitioning of the gut (Fig. 3A′). Observation of the larvae revealed very robust defects. None of the treated embryos formed coelomic pouches or their derivative structures (Fig. 3A′), including the water canal that normally emerges from the left coelomic pouch and connects to the hydropore in the ectodermal wall. FoxY MASO-treated larvae were unable to swallow, although food particles accumulated in their esophagus. Contraction of circumesophageal muscles is responsible for transport of food into the stomach. Rhodamine phalloidin staining of F-actin in 3.5-day-old larvae revealed that these muscles do not form following FoxY MASO injection (Fig. 3B′). Muscle cells

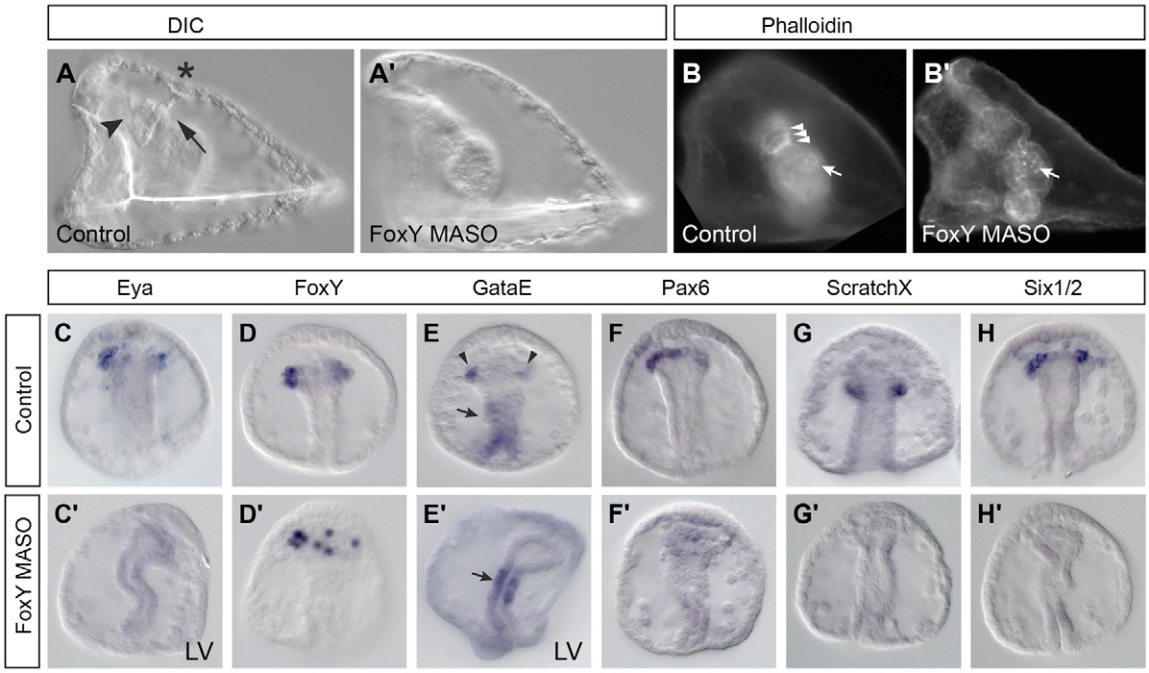

Fig. 3. Loss of FoxY function disrupts coelomic pouch development. (**A**) At 3.5 dpf the left coelomic pouch (arrowhead) lies alongside the esophagus and gives rise to the water canal (arrow) that connects to the hydropore (asterisk) in the ectodermal wall. (**A′**) FoxY MASO injection disrupts the formation of all coelomic pouch-derived structures. (**B**) Rings of muscles form around the esophagus (arrowheads). (**B′**) FoxY MASO application abolishes muscle formation but does not affect Rhodamine phalloidin staining in ciliated gut cells (arrow). (**C**,**C′**,**E-H′**) CPC gene expression is abolished following FoxY MASO treatment. Arrowheads (E) indicate *gataE* expression in CPCs that is lost following treatment; *gataE* expression in the gut is not affected (arrow in E′). (**D**,**D′**) *foxY* expression persists but positioning of *foxY*-positive CPCs is altered. Embryos in C-H′ are 48 hpf and oriented in an aboral view unless otherwise noted. LV, lateral view.

are thought to migrate out of the coelomic epithelium (Burke and Alvarez, 1988), although their exact origin remains unknown. Our results indicate they derive from the group of *foxY*-positive CPC progenitors at the tip of the archenteron. Thus, *foxY* is required for all known functions of NSM Delta signaling, i.e. the specification of CPCs and muscle cells (Materna and Davidson, 2012; Sweet et al., 2002).

At blastula stage (15 hpf), when *foxY* expression is restricted to SMMs, NanoString analysis revealed that no genes are affected by FoxY MASO injection. However, our code set does not contain any genes other than *foxY* that are restricted only to SMMs. A recent study examined the relationship between *foxY* and *nanos* (Song and Wessel, 2012), a stem cell/germ line marker specific to the SMMs until the pluteus stage (Juliano et al., 2010). We supplemented the NanoString data with QPCR data for *nanos* (not shown) and confirmed the previous finding that, at 15 hpf, loss of FoxY function does not affect *nanos* abundance (Song and Wessel, 2012).

If FoxY is the effector of NSM Delta signaling in the CPC progenitors, its knockdown should affect a similar set of genes as observed in our DAPT experiments (Fig. 2A). At 38 and 48 hpf, our quantitative analysis identified a distinct set of genes affected in FoxY morphants that is restricted to CPCs (Fig. 2C; supplementary material Fig. S3A). The changes were indeed similar to those caused by disruption of NSM Delta signaling (Fig. 2A). As in our DAPT treatments, the responsive gene set included all genes known to be specifically and uniquely expressed at the tip of the archenteron at 38 hpf, i.e. *foxC*, *foxF*, *foxY*, *scratchX* and *soxE*. At 48 hpf some differences became apparent: *scratchX* was more strongly affected by FoxY MASO than DAPT treatment. By contrast, *pitx2* was significantly depleted in DAPT-treated embryos but unaffected in FoxY MASO morphants. Although *foxY* is initially expressed in all CPC progenitors, at 48 hpf it becomes strongly biased to CPCs on the left side as a result of *pitx2* repression on the right (see below). The perturbation results thus reflect the progressive regionalization at the archenteron tip. This divergence notwithstanding, the striking agreement at 38 hpf argues that *foxY* is the immediate early effector of Notch signaling within the tip of the archenteron/CPC progenitor population.

We further examined FoxY-responsive genes by WMISH, including *six1/2*, its co-factor *eya*, and *scratchX*, which were undetectable in all FoxY MASO-treated embryos (Fig. 3C,G,H). The transcript levels of *gataE* and *pax6* were only slightly affected in our NanoString analysis (Fig. 2C), but WMISH confirms that the expression of both genes is lost specifically in CPCs (Fig. 3E,F). As mentioned above, *gataE* is strongly expressed in the mid- and hindgut and this expression masks its loss in CPCs in our quantitative analysis (supplementary material Fig. S2B-B″). Similarly, *pax6* is also expressed in the ectoderm (supplementary material Fig. S2C-C″); it becomes predominantly expressed in CPCs only relatively late on (Luo and Su, 2012; Yankura et al., 2010). Our NanoString data showed that *foxY* message is no longer significantly depleted at 48 hpf following FoxY MASO injection. WMISH confirmed that *foxY* is detectable at the tip of the archenteron. However, following FoxY MASO treatment the *foxY*-positive CPCs are dispersed and not restricted to the sides of the archenteron (Fig. 3D,D′). Despite this exception, these results confirm that essentially all of the genes known to be specifically expressed in the CPC compartment are severely depleted when FoxY function is lost.

Pitx2 is the likely effector for establishment of L/R asymmetry

Towards the end of gastrulation, *foxY* expression becomes biased to the left coelomic pouch where eventually the adult rudiment will form. Establishment of L/R asymmetry across the embryo is widely conserved and is dependent on Nodal/Tgfβ signaling (Duboc et al., 2005; Luo and Su, 2012). During embryogenesis, Nodal is first expressed in the oral ectoderm and induces oral cell fate in recipient cells (Duboc et al., 2004; Li et al., 2012; Materna et al., 2013). Later in gastrulation, Nodal expression ceases in the oral ectoderm and is instead activated in the right lateral ectoderm and right coelomic pouch. Interference with this second phase of Nodal signaling results in loss of L/R asymmetry, which is most pronounced in the coelomic pouches where genes restricted to the left side are ectopically expressed on the right, resulting in the formation of two rudiments (Duboc et al., 2005; Luo and Su, 2012).

To identify more comprehensively the gene set responsive to late Nodal signaling, we performed NanoString analysis of embryos treated with the Nodal inhibitor SB431542 at 24 hpf, after the oral/aboral axis is firmly established. Among all 205 genes in our analysis only six were significantly depleted (Fig. 4A; supplementary material Fig. S3B). This included the conserved regulators of L/R asymmetry (*nodal*, *lefty*, *pitx2*) that are expressed in the right ectoderm and coelomic pouch, complementary to *foxY* (Fig. 5B-D) (Duboc et al., 2005; Luo and Su, 2012). *myor2* is depleted following Nodal perturbation, as are *chordin* and the homeobox gene *not*. However, the effect on *chordin* and *not* is due to Nodal signaling within the oral ectoderm, which is still ongoing by the time Nodal inhibitor is added, where these genes are expressed during gastrulation (Li et al., 2012; Materna et al., 2013). Although we cannot exclude the possibility of having missed perturbation effects on genes with more complex expression patterns, the primary candidate as the downstream effector of late Nodal signaling in the establishment of L/R asymmetry is *pitx2*.

Hh signaling triggers coelomic pouch morphogenesis

Hh signaling is known to regulate developmental processes as diverse as patterning, proliferation and morphogenesis (Ingham and McMahon, 2001) and has been linked to the establishment of L/R asymmetry (Tsiairis and McMahon, 2009). In sea urchin embryos the Hh ligand is expressed throughout the endoderm and archenteron starting at the mesenchyme blastula stage (Fig. 1A), concurrent with expression of its downstream effector *gli1* (Walton et al., 2006). The receptors *ptc* and *smo* are present throughout embryogenesis and are expressed prominently at the tip of the archenteron and in the coelomic pouches (Walton et al., 2006; Walton et al., 2009). Experimental activation of Hh signaling has been shown to randomize laterality and cause defects in muscle patterning (Walton et al., 2009), but the function of the endogenous Hh signal with regard to coelomic pouch development has not been studied systematically.

We disrupted Hh signaling by addition of cyclopamine, a highly specific inhibitor of Smo (Chen et al., 2002), to embryos at 22 hpf, prior to the onset of *hh* transcription (Fig. 1A). We determined that a final cyclopamine concentration of 0.5 µM is sufficient to cause reproducible effects (supplementary material Fig. S4) without causing severe developmental delay or death, which were common at 5 µM or higher. Phenotypic inspection revealed several defects, but the most relevant here is the disruption of coelomic pouch morphogenesis. In control embryos the CPC progenitors at the tip of the archenteron split into two groups that relocate laterally to form pouches on either side of the foregut. By contrast, in cyclopamine-treated embryos these cells remained atop the archenteron as a uniform group and formed one pouch-like structure (Fig. 5). Cyclopamine treatment also resulted in failure to form the mouth and in a short gut; whether this is due to improper elongation of the archenteron or defective gut patterning remains to be addressed.

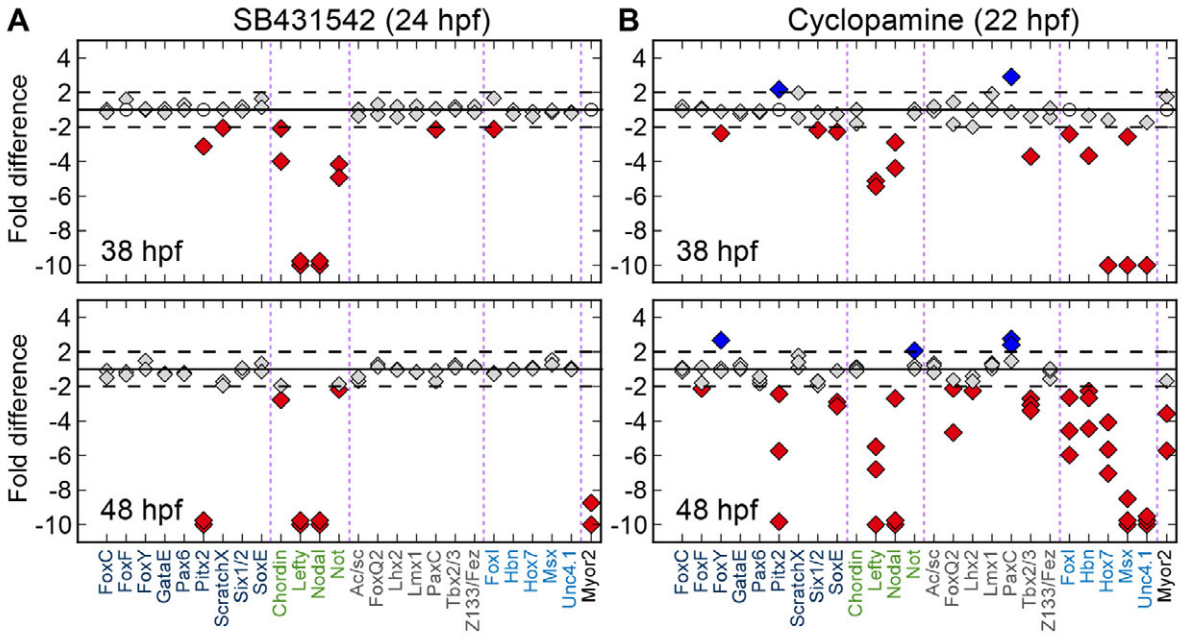

Fig. 4. Effects of Nodal and Hh perturbations on transcript levels. (**A**) Application of the Nodal inhibitor SB431542 causes strongly reduced transcript levels of *lefty*, *nodal*, *pitx2* and *myor2*, but not of endoderm and apical genes. (**B**) Loss of Hh signaling after cyclopamine treatment affects endoderm genes (*foxl*, *hbn*, *hox7*, *msx* and *unc4.1*) in addition to *nodal*, *lefty*, *pitx2* and *myor2*. Symbols and labels as in Fig. 2.

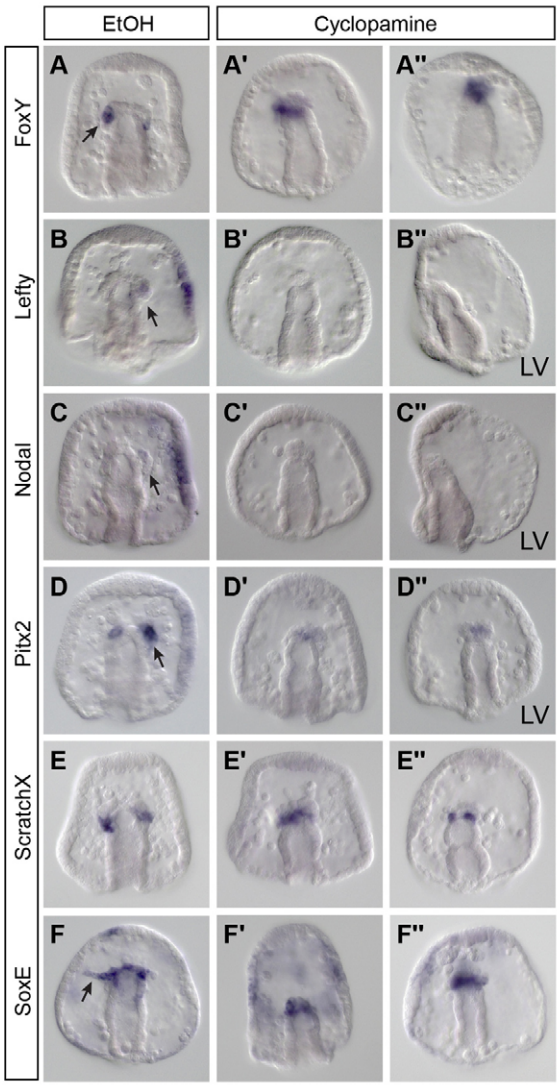

Fig. 5. Spatial effects of Hh perturbation. (**A-A″**) At 66 hpf, *foxY* expression is restricted to the left pouch (arrow). After cyclopamine treatment, *foxY*-expressing CPCs remain at the tip of the archenteron and form one pouch-like structure. (**B-D″**) *lefty*, *nodal* and *pitx2* are expressed in the right lateral ectoderm and right coelomic pouch (arrows in B,C,D); loss of Hh signaling disrupts their expression. (**E-F″**) *scratchX* and *soxE*, like *foxY*, remain strongly expressed following cyclopamine treatment. *soxE* is expressed in the water canal (arrow in F) and in the ciliated band (supplementary material Fig. S2I″). All embryos are oriented in an aboral view unless otherwise noted. EtOH, ethanol control. LV, lateral view.

NanoString analysis of the perturbation effects identified a number of genes reacting strongly to the loss of Hh signaling (Fig. 4B). Some of the strongest effects are found for endoderm genes, highlighting the importance of Hh signaling in gut development. By contrast, and despite the strikingly different morphology, the expression levels of CPC genes were virtually unaltered, except for some minor effects (e.g. *foxF*, *soxE*) (Fig. 4B). *In situ* staining of *foxY* transcript at 66 hpf, more than 30 hours after the pouches separate in controls, revealed strong expression at the tip of the archenteron in agreement with our quantitative analysis (Fig. 5A′,A″). At this time, *foxY* is restricted to the left coelomic pouch in controls (Fig. 5A). Staining of *scratchX* and *soxE* message was strong at the tip of the archenteron, confirming their continued expression following treatment (Fig. 5E′,E″,F′,F″).

One CPC gene strongly depleted in cyclopamine-treated embryos is *pitx2* (Fig. 4B; Fig. 5D′,D″). *nodal* transcript levels were also strongly reduced following cyclopamine treatment, suggesting that the cause for the aberrant *pitx2* expression is loss of Nodal signaling (Fig. 4B). Indeed, *in situ* staining of *nodal* and *lefty* confirmed that their expression, like that of *pitx2*, is lost in the coelomic pouches and also the right lateral ectoderm (Fig. 5B′,B″,C′,C″). In contrast to Nodal perturbation, the *not* gene is unaffected in cyclopamine treatments, supporting the conclusion that loss of Hh signaling specifically affects the late expression phase of *nodal*, which is discontinuous from its earlier expression in the oral ectoderm; it also confirms that the *not* gene is not expressed in coelomic pouches at late gastrulation [it is eventually expressed in the right coelomic pouch during larval development (Luo and Su, 2012)].

In summary, wild-type levels of Hh signaling are required for coelomic pouch morphogenesis, unilateral expression of *nodal* and, as a consequence, for asymmetric gene expression in the coelomic pouches once they have formed.

NICD-Su(H) and Pitx2 are direct regulators of *foxY*

foxY expression is closely linked to that of Delta. To test whether *foxY* is a direct target of Suppressor of Hairless [Su(H)], the downstream effector of D/N signaling that interacts with the Notch intracellular domain (NICD) once it has relocated to the nucleus upon signal reception, we generated reporter constructs of the *foxY* regulatory region. We identified a *foxY* BAC of ~145 kb and inserted the GFP coding region into the second exon by homologous recombination downstream of the start codon to create the *foxY*:GFP BAC reporter (Fig. 6A). This construct replicates endogenous *foxY* expression, albeit in a mosaic fashion as is common in sea urchins (Smith, 2008). GFP expression is first observed in one or two of the SMMs, then in the vegetal plate prior to gastrulation (Fig. 6B), then at the tip of the archenteron, and eventually primarily in the left coelomic pouch (Fig. 6D). Reporter expression in the right pouch occurs at low frequency (see below), as expected based on its weak expression observed in *in situ* stainings.

We amplified successively smaller fragments using the BAC as template and examined reporter expression (Fig. 6A). Construct #3 contains the sequence located between −778 bp upstream of the transcription start site (TSS) and intron 2; its expression was identical to that of the full BAC reporter. Deletion of intron 1 did not alter its expression (Construct #6; Fig. 6C,D). Further shortening at the 5′ end resulted first in equal expression between left and right pouches (Construct #4; Fig. 6E), and then in complete loss of activation (Construct #5). Thus, the region between −400 bp and the TSS contains the regulatory element necessary for expression, and the region between −778 bp and −400 bp contains an element required for the repression of expression in the right coelomic pouch.

We identified a potential Su(H) binding site in the region proximal to the *foxY* TSS (Fig. 7A; supplementary material Fig. S5). To test whether this site is required for activation of *foxY* we mutated it in Construct #3, which was then co-injected with an *alx* reporter that drives GFP expression in skeletogenic cells (Damle and Davidson, 2012) as a marker of integration. Injection of wild-type Construct #3 results in GFP expression within the vegetal plate (100%, 44/44) (Fig. 7C,C′). Expression of Construct #3 is clearly distinguishable from GFP-positive skeletogenic cells within the blastocoel. By contrast, when the Su(H) site was mutated [#3–ΔSu(H)], GFP expression was absent from the vegetal plate

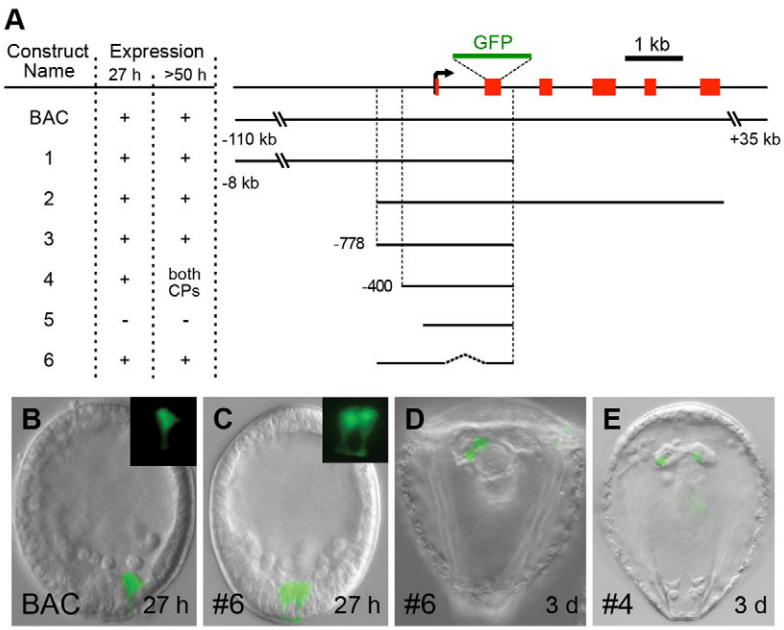

Fig. 6. Identification of regulatory elements driving *foxY* expression. (**A**) *foxY* constructs and their expression. +, greater than 85% (of GFP$^+$ embryos) expressed GFP correctly (SMMs/mesoderm at 27-28 hpf, left coelomic pouch after 50 hpf); –, loss of expression; 'both CPs', expression in both pouches. (**B**) Example of FoxY BAC-GFP expression within the vegetal plate; inset shows the bottle shape of GFP$^+$ cells prior to gastrulation. (**C**) Construct #6 expression is identical to that of the full BAC at 27 hpf. (**D**) Expression of Construct #6 is strongly biased to the left coelomic pouch at 3 dpf. (**E**) Construct #4 drives continuous expression in both pouches.

(95%, 57/60) (Fig. 7D-D″). Similarly, we observed no *foxY* reporter expression during archenteron formation (Fig. 7F,G). Thus, mutation of the Su(H) site within the *foxY* regulatory region confirms that *foxY* is a direct Notch target.

Our data suggest that Nodal might repress *foxY* in the right coelomic pouch via *pitx2*. Unfortunately, two Pitx2 MASOs had toxic side effects resulting in abortive development 24 hours before *pitx2* is first transcribed. We therefore took a more direct approach and set out to identify potential Pitx2 binding sites. Pitx2 binding sites are similar to those of other homeobox factors, most notably Gsc and Otx, with a consensus motif of GGATTA (Berger et al., 2008). However, of these three genes, only *pitx2* is expressed in the coelomic pouches at the appropriate time (Li et al., 2012; Morris et al., 2004); neither *gsc* nor *otx* is affected in our Nodal perturbations. We identified two potential Pitx2 binding sites in the distal *foxY* fragment (Fig. 7A; supplementary material Fig. S5). Mutation of these sites in Construct #3 (#3–ΔPitx2; Fig. 7A) resulted in equal reporter expression in the left and right coelomic pouches, similar to Construct #4 (Fig. 6A; Fig. 7B,B′). In controls, 76% of embryos (40/53) expressed GFP reporter exclusively in the left coelomic pouch, 9% (5/53) in both pouches, and 15% (8/53) exclusively in the right pouch at 3 dpf. We never observed endogenous *foxY* transcript exclusively in the right pouch, indicating that the fraction of embryos expressing GFP reporter on only one side is an overestimate due to mosaic incorporation. By contrast, mutation of both putative Pitx2 binding sites (#3–ΔPitx2) caused a significant shift to the right: 32% of embryos (22/68) showed expression of GFP exclusively in the left pouch, 25% (17/68) in the right pouch, and 43% (29/68) in both pouches. This resembles the bilateral expression of genes otherwise restricted to the left pouch (e.g. *soxE*, *six1/2*) as observed following Nodal perturbation (Duboc et al., 2005; Luo and Su, 2012), and thus provides evidence that *pitx2* is the repressor of *foxY* in the right coelomic pouch.

DISCUSSION

The experiments presented in this work aimed to elucidate the earliest regulatory events required for adult formation in sea urchin larvae. Although much remains to be discovered, our results afford several new and important insights. First, we show that the primary function of NSM Delta expression is to directly activate *foxY* expression in a subset of mesodermal cells that constitute the pool of CPC and muscle cell progenitors. Second, our work demonstrates that *foxY* is the principal effector of the NSM Delta signal. It is essential for specification of the two late mesodermal derivatives and thus constitutes a central node in the regulatory network underlying this process. Third, we find that Hh signaling drives coelomic pouch morphogenesis and that Hh is essential for establishing L/R asymmetry by activating Nodal expression on the right side of the larva. As a consequence, *foxY* is repressed in the right coelomic pouch by Pitx2. Our results show that the initial specification of CPCs, the morphogenesis of the pouches, and the establishment of laterality are three intertwined processes; however, despite their concurrent unfolding they are regulated independently and are thus separable.

foxY expression and mesodermal patterning

The exact origin of late mesodermal derivatives has remained elusive. Fate mapping experiments resolved the origin of pigment and blastocoelar cells within the vegetal plate, but the results were less clear for CPCs and muscle cells (Ruffins and Ettensohn, 1996). The demonstration that NSM Delta is required for specification of both CPCs and muscle cells (Sherwood and McClay, 1999; Sweet et al., 2002) led to the identification of *foxY* as a potential downstream effector (Materna and Davidson, 2012). As our expression analysis shows, *foxY* is likely to be the first transcription factor specifically expressed in the entire veg2-derived progenitor pool of CPCs and muscle cells. At early mesenchyme blastula stage, *delta* transcript is present throughout the NSM (Materna and Davidson, 2012; Sweet et al., 2002; Walton et al., 2006), including the cells directly adjacent to the SMMs that go on to activate *foxY* expression. This contradicts the idea that Delta presentation and active Notch signaling are mutually exclusive (del Álamo et al., 2011) and suggests that Delta expression might be more dynamic within the NSM than currently assumed. The exceedingly low transcript levels of *delta* during its expression in NSM (Materna et al., 2010) and the rearrangements following ingression of pigment

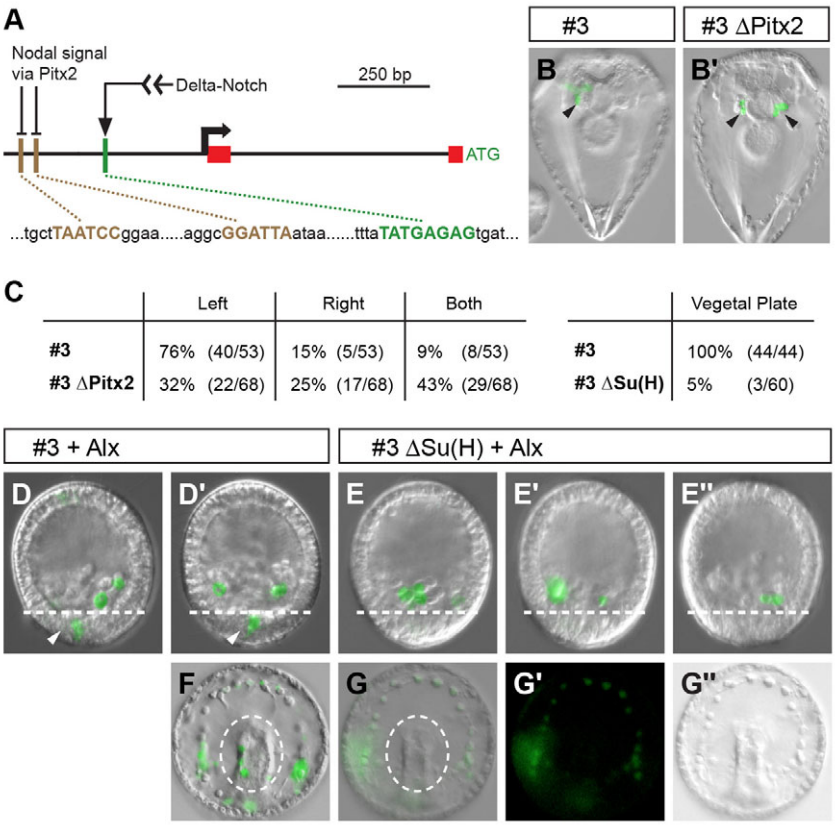

Fig. 7. Identification of functional binding sites in the *foxY* regulatory region. (**A**) Location of the tested putative Pitx2 (brown) and Su(H) (green) binding sites upstream of the *foxY* transcription start site (bent arrow). (**B**,**B′**) Construct #3 shows reporter expression (arrowhead) in the left coelomic pouch at 3 dpf. Mutation of the homeobox sites (#3–ΔPitx2) results in robust expression in both coelomic pouches. (**C**) Frequencies of spatial expression of Construct #3 versus #3–ΔPitx2 at 3 dpf and of Construct #3 versus #3–ΔSu(H) at 27-28 hpf. (**D**,**D′**,**F**) Construct #3 is expressed first within the vegetal plate (arrowhead) at 27-28 hpf and at the tip of the archenteron at 48 hpf (within dashed circle in F). Co-injected Alx BAC-GFP is expressed in ingressed skeletogenic cells (above dashed line). (**E-E″**,**G-G″**) Disruption of the Su(H) site [#3–ΔSu(H)] abolishes reporter expression in the vegetal plate and in the archenteron (within dashed circle in G); Alx BAC-GFP expression in skeletogenic cells is unaffected. The GFP channel is shown in G′, DIC in G″.

and blastocoelar cells make disentangling the different mesodermal lineages challenging.

The dramatic phenotype caused by FoxY MASO injection, i.e. the complete lack of coelomic pouches as well as muscle cells, demonstrates the importance of FoxY. Our observation that expression of essentially all CPC genes is abolished identifies *foxY* as the linchpin in the regulatory network underlying the specification of CPCs. Exceptions are few: *pitx2* is affected only in D/N perturbations but not following injection of FoxY MASO; but this is not surprising given the likely role of Pitx2 as the repressor of *foxY* in the right coelomic pouch. Nevertheless, the fact that *pitx2* indirectly requires D/N signaling but not FoxY indicates that the functions of NSM Delta signaling and FoxY, although largely overlapping, are not perfectly congruent. The transient expression of Delta in the NSM requires that *foxY* receives additional inputs to assure its continued expression. *foxY* is likely to be part of a positive-feedback loop involving genes that it first activates, as is common for pioneering transcription factors establishing a new regulatory state (Davidson, 2010). Such recursive wiring might be the cause of the mostly normal, albeit low, transcript levels of *foxY* following its own perturbation at late gastrulation, i.e. only after a long delay. Additionally, *foxY* might also be activated by Bmp/Tgfβ signaling, as has been suggested for other CPC genes (Luo and Su, 2012). Nevertheless, restriction of *foxY* expression to the left side, where it remains expressed (Ransick et al., 2002), is one of the first events in the progressive regionalization at the tip of the archenteron and presages where the adult rudiment will form. Although muscle cells are derived from the same group of *foxY*-positive progenitor cells, they give rise to between 20 and 40 fully differentiated cells in grown larvae (Burke and Alvarez, 1988; Cox et al., 1986). By contrast, the CPCs are a major contributor to the adult; at metamorphosis, their descendants number in the tens of thousands.

Coelomic pouch morphogenesis and symmetry breaking

The separation of CPC progenitors and their relocation to the sides of the foregut is dependent on Hh signaling. This morphogenetic process resembles the separation of midline structures in vertebrates, which is strongly dependent on Hh signaling (Schachter and Krauss, 2008). Improper regulation of Hh signaling leads to severe defects such as cyclopia and incomplete separation of brain structures (Roessler et al., 1996). In sea urchins, loss of Smo activation results in the formation of only one centrally located coelomic pouch. However, none of the transcription factors expressed specifically at the tip of the archenteron is affected by loss of Hh signaling. The only exception in our dataset is *pitx2* due to interference with late Nodal expression. Thus, the CPCs now positioned atop the foregut display the regulatory state that is normally reserved for the left coelomic pouch only. Additional Hh-responsive transcription factors might await discovery but Hh signaling may also directly regulate morphogenetic effector genes, such as those encoding cell motility or adhesion molecules. When misregulated, these genes cause similar craniofacial defects as loss of Hh signaling (Chen et al., 2006).

Hh signaling is required for the establishment of laterality in sea urchins

Loss of Hh signaling causes failure to activate *nodal* transcription in the right coelomic pouch and the right lateral ectoderm. The importance of Nodal signaling in L/R asymmetry has been studied extensively (Bessodes et al., 2012; Duboc et al., 2005; Luo and Su,

2012; Nakamura and Hamada, 2012) and a close link between Hh and Nodal signaling is well established (Zhang et al., 2001). Nevertheless, how the two signaling systems relate to each other mechanistically remains unknown. Laterality defects in mice caused by loss of Hh signaling can be rescued by expression of a constitutively active Smo receptor in lateral plate mesoderm resulting in unilateral expression of *nodal* (Tsiairis and McMahon, 2009). In sea urchins, overexpression of a constitutively active Smo receptor randomizes the position of the adult rudiment (Walton et al., 2009). It has recently been shown that unilateral expression of Nodal at the archenteron tip, and thus in close proximity to the Hh source, determines the sidedness of Nodal expression in the ectoderm (Bessodes et al., 2012). However, in contrast to our Hh perturbations, disruption of Nodal signaling specifically within the archenteron leads to randomization of *nodal* transcription in the ectoderm and not to loss of expression; whether Hh itself is received in the ectoderm is currently unknown. Regardless, although the initial cause of symmetry breaking remains elusive, it is well recognized that Nodal signaling is part of the conserved downstream mechanism establishing laterality across the embryo (Duboc et al., 2005; Grande and Patel, 2009; Nakamura and Hamada, 2012). Our experiments demonstrate that in sea urchins this function includes repression of *foxY* in the right coelomic pouch by Pitx2, thus confining *foxY* expression, and adult rudiment formation, to the left side.

CPCs as multipotent progenitors

Coelomic pouches are a conserved feature of echinoderm embryos (Chia and Walker, 1991; Pearse and Cameron, 1991), but whether the molecular mechanisms controlling their formation are conserved is currently unknown. Nevertheless, in the distantly related starfish *Patiria miniata*, coelomic pouch formation is dependent on D/N signaling within the mesoderm just as it is in euechinoids (V. Hinman, personal communication). Whether starfish and other echinoderms possess a *foxY* ortholog that is employed downstream of D/N signaling is an open question.

A second conserved feature is the localized expression of Vasa protein. Although initially localized to SMMs, Vasa eventually becomes expressed throughout the coelomic pouches (Juliano et al., 2010). Despite its connection to germ cell specification, recent evidence indicates that Vasa is more broadly connected to pluripotency (Gustafson and Wessel, 2010) and is expressed in mammalian embryonic stem cells (Ingham and McMahon, 2001; Ramalho-Santos et al., 2002) and in adult stem cells in planarians and *Hydra* (Rebscher et al., 2008). In polychaete annelids, Vasa is expressed throughout the mesodermal posterior growth zone, a group of multipotent stem cells that, similar to the coelomic pouches in echinoderms, gives rise to adult structures and germ cells (Rebscher et al., 2007).

Coelomic pouch development thus provides a unique opportunity to understand how developmental potency is maintained throughout successive patterning events in cells that are embedded in an environment that otherwise promotes rapid differentiation.

Acknowledgements
We are grateful for support and advice from Eric Davidson in whose laboratory most of the work was performed. Many thanks to Celina Juliano and Andy Cameron for numerous insights and to Gary Wessel for Vasa antibody.

Funding
This work was supported by the National Institutes of Health [grant HD-037105 to Eric Davidson and 1P30GM092374-01 to J.S.]; and a California Institute for Regenerative Medicine (CIRM) fellowship to J.S. Deposited in PMC for release after 12 months.

Competing interests statement
The authors declare no competing financial interests.

Supplementary material
Supplementary material available online at
http://dev.biologists.org/lookup/suppl/doi:10.1242/dev.091157/-/DC1

References

Arenas-Mena, C. (2010). Indirect development, transdifferentiation and the macroregulatory evolution of metazoans. *Philos. Trans. R. Soc. Lond. B Biol. Sci.* **365**, 653-669.
Berger, M. F., Badis, G., Gehrke, A. R., Talukder, S., Philippakis, A. A., Peña-Castillo, L., Alleyne, T. M., Mnaimneh, S., Botvinnik, O. B., Chan, E. T. et al. (2008). Variation in homeodomain DNA binding revealed by high-resolution analysis of sequence preferences. *Cell* **133**, 1266-1276.
Bessodes, N., Haillot, E., Duboc, V., Röttinger, E., Lahaye, F. and Lepage, T. (2012). Reciprocal signaling between the ectoderm and a mesendodermal left-right organizer directs left-right determination in the sea urchin embryo. *PLoS Genet.* **8**, e1003121.
Burke, R. D. and Alvarez, C. M. (1988). Development of the esophageal muscles in embryos of the sea urchin Strongylocentrotus purpuratus. *Cell Tissue Res.* **252**, 411-417.
Cameron, R. A., Britten, R. J. and Davidson, E. H. (1989). Expression of two actin genes during larval development in the sea urchin Strongylocentrotus purpuratus. *Mol. Reprod. Dev.* **1**, 149-155.
Cameron, R. A., Fraser, S. E., Britten, R. J. and Davidson, E. H. (1991). Macromere cell fates during sea urchin development. *Development* **113**, 1085-1091.
Chen, J. K., Taipale, J., Cooper, M. K. and Beachy, P. A. (2002). Inhibition of Hedgehog signaling by direct binding of cyclopamine to Smoothened. *Genes Dev.* **16**, 2743-2748.
Chen, L., Liao, G., Yang, L., Campbell, K., Nakafuku, M., Kuan, C.-Y. and Zheng, Y. (2006). Cdc42 deficiency causes Sonic hedgehog-independent holoprosencephaly. *Proc. Natl. Acad. Sci. USA* **103**, 16520-16525.
Chia, F. S. and Walker, C. W. (1991). Echinodermata: asteroidea. In *Reproduction of Marine Invertebrates, Echinoderms and Lophophorates*, Vol. 4 (ed. A. C. Giese, J. S. Pearse and V. B. Pearse), pp. 301-353. Pacific Grove, CA: Boxwood Press.
Cox, K. H., Angerer, L. M., Lee, J. J., Davidson, E. H. and Angerer, R. C. (1986). Cell lineage-specific programs of expression of multiple actin genes during sea urchin embryogenesis. *J. Mol. Biol.* **188**, 159-172.
Damle, S. S. and Davidson, E. H. (2012). Synthetic in vivo validation of gene network circuitry. *Proc. Natl. Acad. Sci. USA* **109**, 1548-1553.
Davidson, E. H. (2010). Emerging properties of animal gene regulatory networks. *Nature* **468**, 911-920.
del Álamo, D., Rouault, H. and Schweisguth, F. (2011). Mechanism and significance of cis-inhibition in Notch signalling. *Curr. Biol.* **21**, R40-R47.
Duboc, V., Röttinger, E., Besnardeau, L. and Lepage, T. (2004). Nodal and BMP2/4 signaling organizes the oral-aboral axis of the sea urchin embryo. *Dev. Cell* **6**, 397-410.
Duboc, V., Röttinger, E., Lapraz, F., Besnardeau, L. and Lepage, T. (2005). Left-right asymmetry in the sea urchin embryo is regulated by nodal signaling on the right side. *Dev. Cell* **9**, 147-158.
Geiss, G., Bumgarner, R., Birditt, B., Dahl, T., Dowidar, N., Dunaway, D., Fell, H., Ferree, S., George R., Grogan, T. et al. (2008). Direct multiplexed measurement of gene expression with color-coded probe pairs. *Nat. Biotechnol.* **26**, 317-325.
Grande, C. and Patel, N. H. (2009). Lophotrochozoa get into the game: the nodal pathway and left/right asymmetry in bilateria. *Cold Spring Harb. Symp. Quant. Biol.* **74**, 281-287.
Gustafson, E. A. and Wessel, G. M. (2010). Vasa genes: emerging roles in the germ line and in multipotent cells. *BioEssays* **32**, 626-637.
Howard-Ashby, M., Materna, S. C., Brown, C. T., Chen, L., Cameron, R. A. and Davidson, E. H. (2006a). Gene families encoding transcription factors expressed in early development of Strongylocentrotus purpuratus. *Dev. Biol.* **300**, 90-107.
Howard-Ashby, M., Materna, S. C., Brown, C. T., Chen, L., Cameron, R. A. and Davidson, E. H. (2006b). Identification and characterization of homeobox transcription factor genes in Strongylocentrotus purpuratus, and their expression in embryonic development. *Dev. Biol.* **300**, 74-89.
Ingham, P. W. and McMahon, A. P. (2001). Hedgehog signaling in animal development: paradigms and principles. *Genes Dev.* **15**, 3059-3087.
Juliano, C. E., Yajima, M. and Wessel, G. M. (2010). Nanos functions to maintain the fate of the small micromere lineage in the sea urchin embryo. *Dev. Biol.* **337**, 220-232.
Li, E., Materna, S. C. and Davidson, E. H. (2012). Direct and indirect control of oral ectoderm regulatory gene expression by Nodal signaling in the sea urchin embryo. *Dev. Biol.* **369**, 377-385.
Luo, Y. J. and Su, Y. H. (2012). Opposing nodal and BMP signals regulate left-right asymmetry in the sea urchin larva. *PLoS Biol.* **10**, e1001402.

Materna, S. C. and Davidson, E. H. (2012). A comprehensive analysis of Delta signaling in pre-gastrular sea urchin embryos. *Dev. Biol.* **364**, 77-87.
Materna, S. C. and Oliveri, P. (2008). A protocol for unraveling gene regulatory networks. *Nat. Protoc.* **3**, 1876-1887.
Materna, S. C., Howard-Ashby, M., Gray, R. and Davidson, E. H. (2006). The C2H2 zinc finger genes of Strongylocentrotus purpuratus and their expression in embryonic development. *Dev. Biol.* **300**, 108-120.
Materna, S. C., Nam, J. and Davidson, E. H. (2010). High accuracy, high-resolution prevalence measurement for the majority of locally expressed regulatory genes in early sea urchin development. *Gene Expr. Patterns* **10**, 177-184.
Materna, S. C., Ransick, A., Li, E. and Davidson, E. H. (2013). Diversification of oral and aboral mesodermal regulatory states in pregastrular sea urchin embryos. *Dev. Biol.* **375**, 92-104.
Minelli, A. (2009). *Perspectives in Animal Phylogeny and Evolution*. New York, USA: Oxford University Press.
Morris, V. B., Zhao, J.-T., Shearman, D. C. A., Byrne, M. and Frommer, M. (2004). Expression of an Otx gene in the adult rudiment and the developing central nervous system in the vestibula larva of the sea urchin Holopneustes purpurescens. *Int. J. Dev. Biol.* **48**, 17-22.
Nakamura, T. and Hamada, H. (2012). Left-right patterning: conserved and divergent mechanisms. *Development* **139**, 3257-3262.
Pearse, J. S. and Cameron, R. A. (1991). Echinodermata: Echinoidea. In *Reproduction of Marine Invertebrates, Echinoderms and Lophophorates*, Vol. 4 (ed. A. C. Giese, J. S. Pearse and V. B. Pearse), pp. 513-662. Pacific Grove, CA: Boxwood Press.
Pehrson, J. R. and Cohen, L. H. (1986). The fate of the small micromeres in sea urchin development. *Dev. Biol.* **113**, 522-526.
Poustka, A. J., Kühn, A., Groth, D., Weise, V., Yaguchi, S., Burke, R. D., Herwig, R., Lehrach, H. and Panopoulou, G. (2007). A global view of gene expression in lithium and zinc treated sea urchin embryos: new components of gene regulatory networks. *Genome Biol.* **8**, R85.
Ramalho-Santos, M., Yoon, S., Matsuzaki, Y., Mulligan, R. C. and Melton, D. A. (2002). 'Stemness': transcriptional profiling of embryonic and adult stem cells. *Science* **298**, 597-600.
Ransick, A. and Davidson, E. H. (2006). cis-regulatory processing of Notch signaling input to the sea urchin glial cells missing gene during mesoderm specification. *Dev. Biol.* **297**, 587-602.
Ransick, A., Rast, J. P., Minokawa, T., Calestani, C. and Davidson, E. H. (2002). New early zygotic regulators expressed in endomesoderm of sea urchin embryos discovered by differential array hybridization. *Dev. Biol.* **246**, 132-147.
Rebscher, N., Zelada-González, F., Banisch, T. U., Raible, F. and Arendt, D. (2007). Vasa unveils a common origin of germ cells and of somatic stem cells from the posterior growth zone in the polychaete Platynereis dumerilii. *Dev. Biol.* **306**, 599-611.
Rebscher, N., Volk, C., Teo, R. and Plickert, G. (2008). The germ plasm component Vasa allows tracing of the interstitial stem cells in the cnidarian Hydractinia echinata. *Dev. Dyn.* **237**, 1736-1745.
Roessler, E., Belloni, E., Gaudenz, K., Jay, P., Berta, P., Scherer, S. W., Tsui, L. C. and Muenke, M. (1996). Mutations in the human sonic hedgehog gene cause holoprosencephaly. *Nat. Genet.* **14**, 357-360.
Ruffins, S. W. and Ettensohn, C. A. (1996). A fate map of the vegetal plate of the sea urchin (Lytechinus variegatus) mesenchyme blastula. *Development* **122**, 253-263.
Schachter, K. A. and Krauss, R. S. (2008). Murine models of holoprosencephaly. *Curr. Top. Dev. Biol.* **84**, 139-170.
Sherwood, D. R. and McClay, D. R. (1999). LvNotch signaling mediates secondary mesenchyme specification in the sea urchin embryo. *Development* **126**, 1703-1713.
Smith, J. (2008). A protocol describing the principles of cis-regulatory analysis in the sea urchin. *Nat. Protoc.* **3**, 710-718.
Smith, J. and Davidson, E. H. (2008). Gene regulatory network subcircuit controlling a dynamic spatial pattern of signaling in the sea urchin embryo. *Proc. Natl. Acad. Sci. USA* **105**, 20089-20094.
Song, J. L. and Wessel, G. M. (2012). The forkhead transcription factor FoxY regulates Nanos. *Mol. Reprod. Dev.* **79**, 680-688.
Spradling, A., Fuller, M. T., Braun, R. E. and Yoshida, S. (2011). Germline stem cells. *Cold Spring Harb. Perspect. Biol.* **3**, a002642.
Strickland, L., von Dassow, G., Ellenberg, J., Foe, V., Lenart, P. and Burgess, D. (2004). Light microscopy of echinoderm embryos. *Methods Cell Biol.* **74**, 371-409.
Sweet, H. C., Gehring, M. and Ettensohn, C. A. (2002). LvDelta is a mesoderm-inducing signal in the sea urchin embryo and can endow blastomeres with organizer-like properties. *Development* **129**, 1945-1955.
Tanaka, S. and Dan, K. (1990). Study of the lineage and cell cycle of small micromeres in embryos of the sea urchin, Hemicentrotus pulcherrimus. *Dev. Growth Differ.* **32**, 145-156.
Tsiairis, C. D. and McMahon, A. P. (2009). An Hh-dependent pathway in lateral plate mesoderm enables the generation of left/right asymmetry. *Curr. Biol.* **19**, 1912-1917.
Tu, Q., Brown, C. T., Davidson, E. H. and Oliveri, P. (2006). Sea urchin Forkhead gene family: phylogeny and embryonic expression. *Dev. Biol.* **300**, 49-62.
Voronina, E., Lopez, M., Juliano, C. E., Gustafson, E., Song, J. L., Extavour, C., George, S., Oliveri, P., McClay, D. and Wessel, G. (2008). Vasa protein expression is restricted to the small micromeres of the sea urchin, but is inducible in other lineages early in development. *Dev. Biol.* **314**, 276-286.
Walton, K. D., Croce, J. C., Glenn, T. D., Wu, S.-Y. and McClay, D. R. (2006). Genomics and expression profiles of the Hedgehog and Notch signaling pathways in sea urchin development. *Dev. Biol.* **300**, 153-164.
Walton, K. D., Warner, J., Hertzler, P. H. and McClay, D. R. (2009). Hedgehog signaling patterns mesoderm in the sea urchin. *Dev. Biol.* **331**, 26-37.
Yajima, M. and Wessel, G. M. (2011). Small micromeres contribute to the germline in the sea urchin. *Development* **138**, 237-243.
Yankura, K. A., Martik, M. L., Jennings, C. K. and Hinman, V. F. (2010). Uncoupling of complex regulatory patterning during evolution of larval development in echinoderms. *BMC Biol.* **8**, 143.
Zhang, X. M., Ramalho-Santos, M. and McMahon, A. P. (2001). Smoothened mutants reveal redundant roles for Shh and Ihh signaling including regulation of L/R symmetry by the mouse node. *Cell* **106**, 781-792.

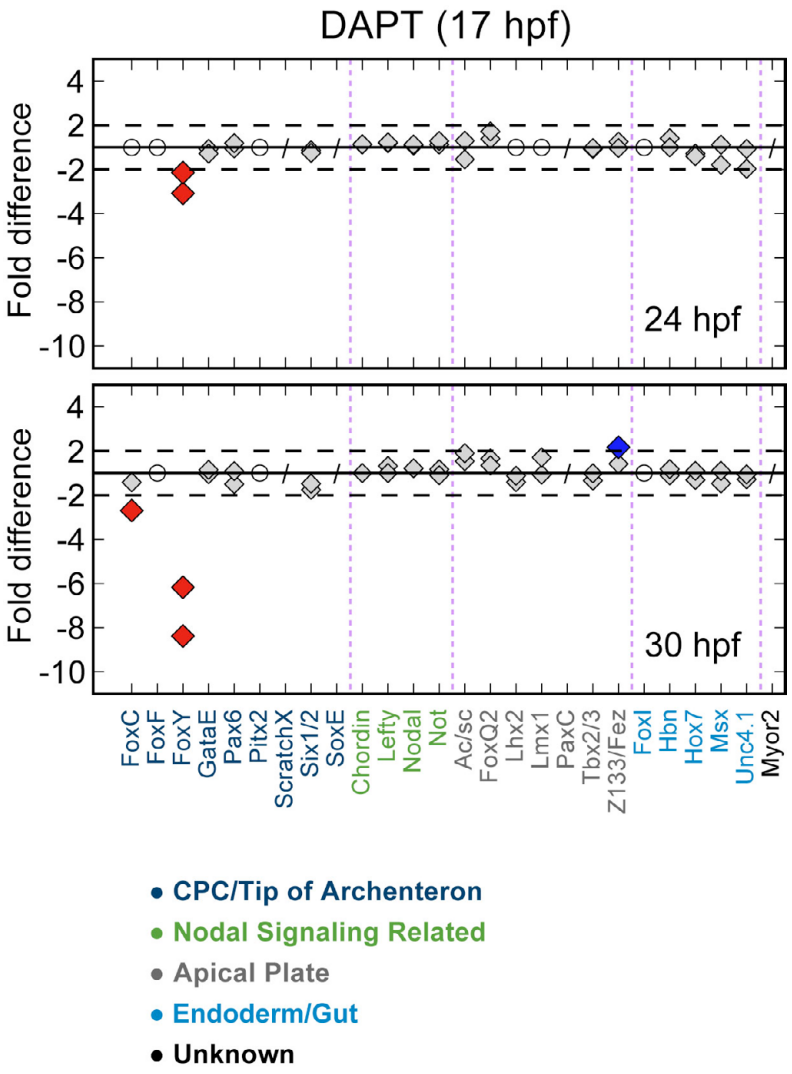

Fig. S1. Effects of Delta/Notch perturbations on transcript levels at 24 hpf and 30 hpf for the same selection of genes as shown in Fig. 2. DAPT treatment at 17 hpf causes strong and consistent depletion of only *foxY* among the 182 genes included in this dataset. The data are reformatted from Materna and Davidson (Materna and Davidson, 2012). Each diamond represents a single experiment; red indicates a significant reduction, blue an increase, and gray no significant change of transcript levels following treatment. Genes not significantly transcribed in experiment and control are marked with an open circle. We estimated transcript levels by comparing our data with prior absolute measurements (Materna et al., 2010). A level of 25 transcripts/embryo was chosen as significant expression. Genes not tested are marked with a solidus. Black dashed lines indicate the threshold for significant changes following perturbation.

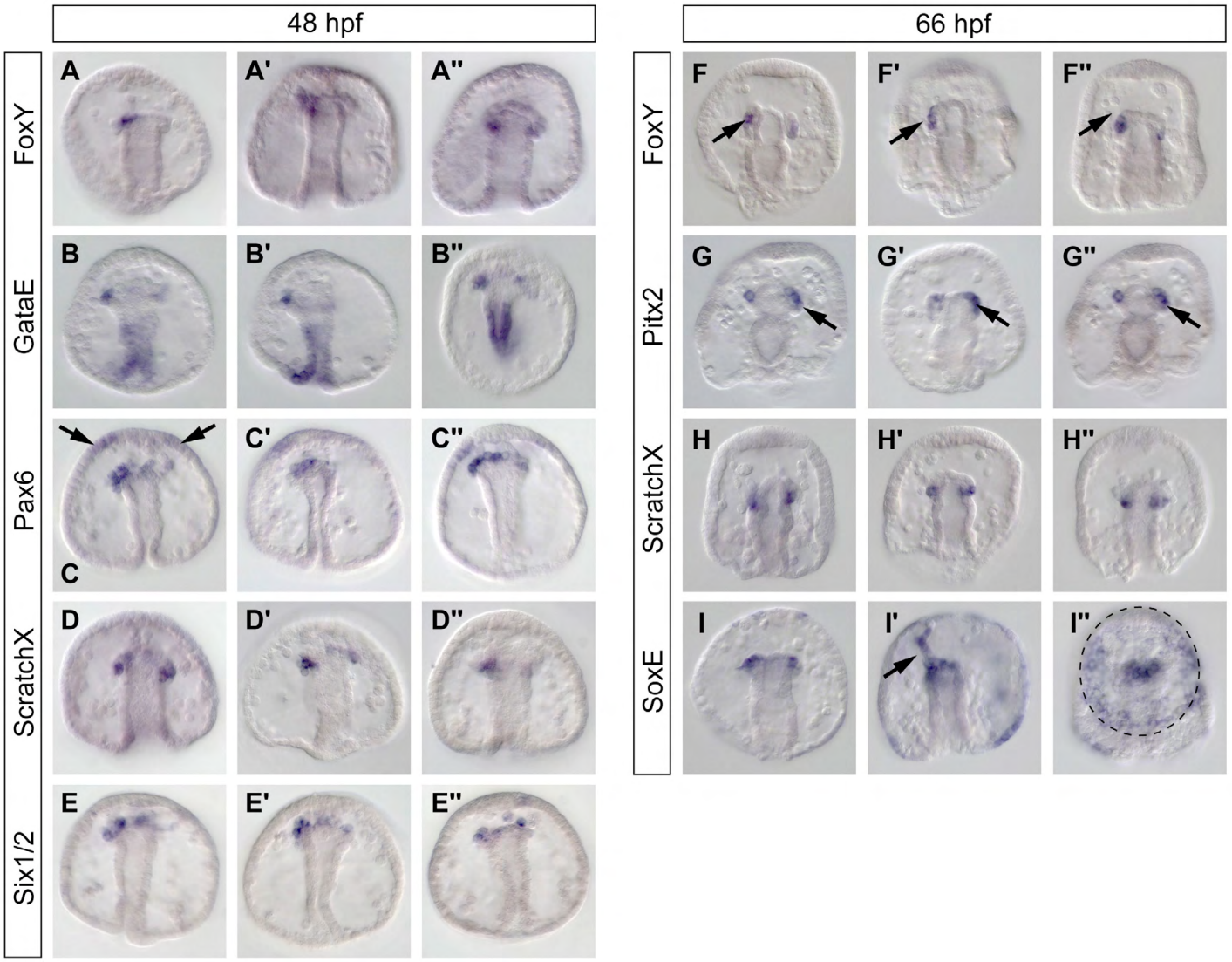

Fig. S2. Additional spatial expression patterns of genes with a specific coelomic pouch expression compartment. (**A-A″**,**F-F″**) *foxY* expression is biased to the left side at 48 hpf, but becomes restricted to the left side after 66 hpf (arrows in F-F″). (**B-B″**) *gataE* is expressed in the gut and the coelomic pouches, and is biased to the left side. (**C-C″**) *pax6* is expressed at the tip of the archenteron, but also in the ectoderm surrounding the apical plate (arrows in C). (**D-D″**,**H-H″**) *scratchX* is expressed in both pouches and remains bilaterally expressed until at least 3 dpf. (**E-E″**) At 48 hpf *six1/2* is expressed at the tip of the archenteron. (**G-G″**) *pitx2* is preferentially expressed in the right coelomic pouch (arrow). *pitx2* and *foxY* expression patterns are complementary; overlap is minimal at best (compare G-G″ with F-F″). (**I-I″**) *soxE* is expressed in the coelomic pouches and the water canal as it emerges from the left coelomic pouch (arrow in I′). It has a second expression domain in the ciliated band (dashed line in I″).

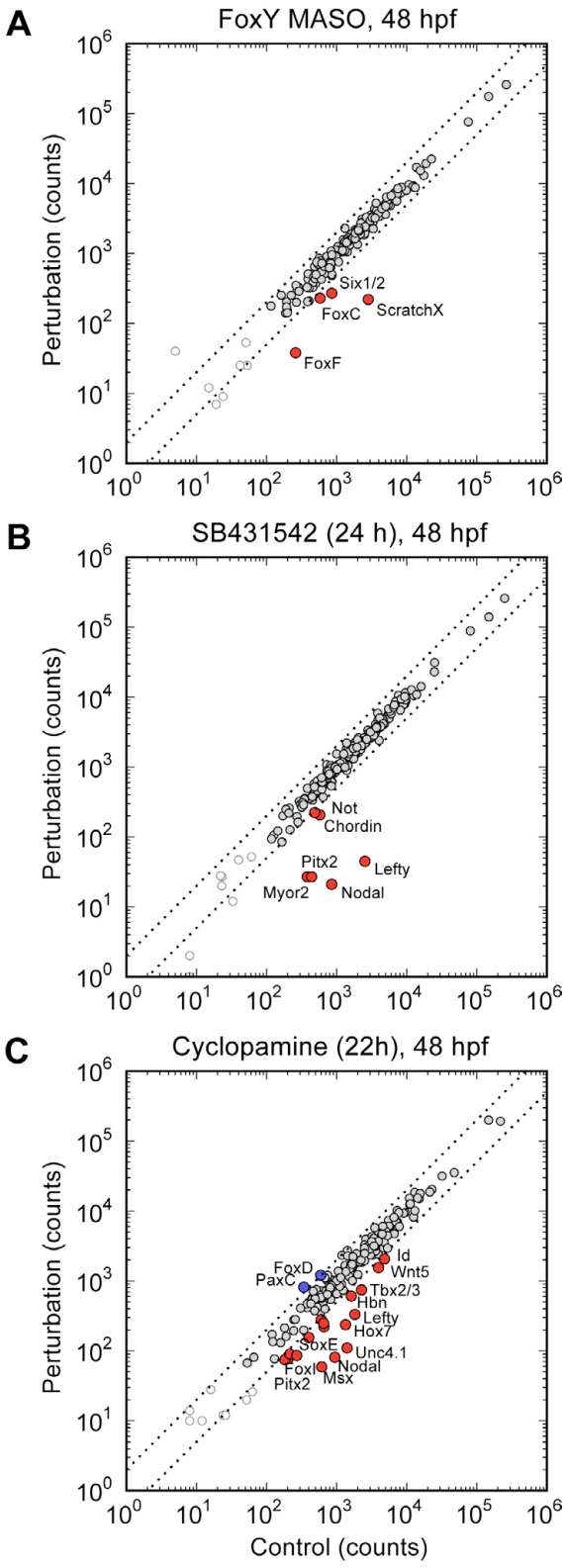

Fig. S3. Global evaluation of perturbation effects by transcript quantification. RNA from treated embryos was extracted and quantified using the NanoString nCounter and the resulting counts were normalized. Counts from perturbed embryos were plotted against those of control embryos. (**A**) FoxY MASO injection at fertilization causes depletion of transcript levels for genes specifically expressed in the coelomic pouch progenitors. Out of 205 genes only a few, none of them outside the *foxY* expression compartment, are affected by the perturbation, indicating that the MASO does not cause nonspecific delays in development. (**B**) Nodal perturbation by addition of the inhibitor SB431542 at 24 hpf causes lower transcript levels of only six genes included in the NanoString code set. (**C**) Disruption of Hh by application of cyclopamine has more widespread effects and also causes depletion of several endoderm genes. Labels for some weakly affected genes that were not substantiated in repeat experiments were left out of C for clarity. The dotted lines indicate a threshold of 2-fold change. A red dot indicates significant depletion following treatment, a blue dot a significant increase, and a gray dot indicates no significant change. Genes present with ~25 transcripts or fewer per embryo are marked with an open circle; transcription levels were estimated from prior absolute measurements (Materna et al., 2010).

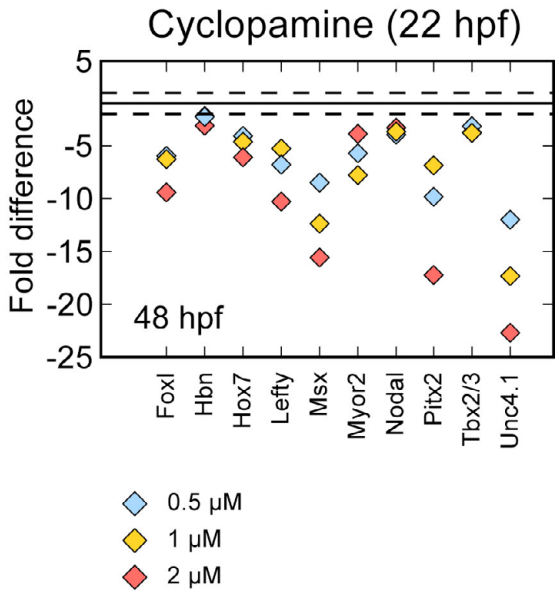

Fig. S4. Effects of cyclopamine treatment are dose dependent. Sea urchin embryos from the same batch were treated with the indicated concentrations of cyclopamine to disrupt Hh signaling. RNA was extracted and quantified with the NanoString nCounter and fold differences were calculated between controls (ethanol only) and cyclopamine-treated embryos. This plot shows the genes that are most strongly affected by the perturbation (compare with Fig. 4B and Fig. S3C). In our experiments, cyclopamine concentrations of 5 µM and higher caused severe developmental delays and death.

FoxY Construct #3 upstream region (-778 to ATG/GFP in second exon)

TTCGCAGGCTAGAGACACCTCTCTGCTTAATCCGGAAGCTTAAACAAAGAGCCCTCATTGTCAATGGTGTAGTG
TACGAGGCGGATTAATAAATCCAATTAGAAGGGTATCACCAGGCGTGGGAAAAGGAATGGGTCTGACTTGGCTA
GTCTTATCATTTCATCATCAGACCGTTTTGAAAACAATCCATAATAGATTAGAGTCAATAAATTAGACAGATGA
TAAAATGGGTCTTGATTTGCTATAGATCGTTGGCATACGCCATGCATTGGGTATGATGTCTTTTAAGCCATTCG
AACAAAACACTATATATGCAATCATGCACAATCTGATTTCTTCTTCTCTGTCTTTCTCTCCATGCCCCCTCCCC
GCCCCCCCCCCCCTCTCTCTCTCCTCTATCTCAGAGAGTTTCTGTCTCTATATAGAAACTCTCTAGACATTA
TTTGAAACTTCTATGATTGTACAATATGCGTTTGGACAATTGTCATGTTTGTGAATTTTGAGTATCATTTTTAT
ATGAGAGTGATATTTTGTTGATCGACGGTATGATTGAAAAAGATCAACTTGGTCTGATTTCAAAGACTACCATA
TAGAAAAAGATTGTTCGCGCATGCGTCGCCCTGATCCTTTCTTTCGCATCTCGATTACGTAACACCTCGCTCTC
CTGTAATTGGCTTAGAGTTGGTAAGAACGGTGAGAACAGATCAGGTATAAAGTAAGATAGAAGTCCGATGAAGA
AGCTTATCTTGCTCAAGACCTCTGAACTGGAAACATTGCTGCACTGACTCTGCCTACATACCCAGCTTCACAAA
TCTCGCCTCATCGATTGCCTTACTCCTCATTTTCCATACCATTTGTAGGTGAGTATCTCACGTTAAATTGTAAT
ATTATCTGTCGTAATAATGATTTGACTCCATTTCTGTAGTACTCGTGGTGATTTAAGTGTTTGGAGCGAATGTT
AGTCTTGTTGGTTGAATGGTGACTTGCGTTTGTTTTCTTATCGATGAGAGGGGAATTCGTGTGAAGGGTTTTTA
AATTACAGATGCCAATATTCCAATATCAGTTCAGCTTAACATCCAGTAAAACCAGTAATATACAATATACAAAC
ATATCTCATCAATTTCTTTAATATGTTCAATTAGGCATGTAAATTACTCAGGGAACATCTATAGTATATAGGCC
TACTTCGGAATATTCTTTTGTCTTCTTGATTATGAACCATTCTGGCCAGAAAGATATACGGCTAGGCCCAGAGC
ATGATCAGGTATATTTTTGTTCTGTTATACGTGAGCTTTGAGTGTCGTACATAATATATGTATATTCTTTGTAA
ATATTTTTGCGTGGAATTCGTTTGCCCCAAAATGATTATATTAGTGTTGGTTTTATGAATGTCTATACAATCGA
TACCTTTTTATGATTGTTATTCATGAATCAAAGATGAAATAAAGAAGGAAAAAATGAACCCGTTGTTTTCCGGA
GATGTGGGAGGTAAATTTATGACCAAAAATCTACTTGTCTTTTTTTCACTTTTCATGAATAGTGTTCTGCACTT
GGAGCCATGAGCAAGGGCGAGGAACTGTTCACTGGCG...

- Pitx2 binding sites
- Start of Construct #4
- Su(H) binding sites
- Exon
- Splice Site
- Start codon
- GFP sequence

Fig. S5. Annotated sequence of the regulatory region upstream of the *foxY* transcription start site. This sequence corresponds to the region contained in Construct 3; Construct 4 is nested within, starting at position 379 (marked in blue). 5′-(C/T)(A/G)TG(A/G)GA(A/G/T)-3′ was used to identify candidate Su(H) sites (Ransick and Davidson, 2006). The TG at positions 3 and 4, and the GA at positions 6 and 7, were mutated to CA and AG. We used the sequence 5′-GGATTA-3′ to identify candidate Pitx2 target sites, and mutated 5′-GATT-3′ to 5′-AGCC-3′.

Table S1. Primers for WMISH templates and QPCR

Gene	Forward primer	Reverse primer	Use	Accession No.
eya	GTATTGGAAGAGGGCGTCAA	AGGAGGGGTGGATAGCATCT	WMISH template	SPU_013869
foxY	ACTGGATGATCAACCCAAGC	AGAAACCTTTGGTGGTGTCG	WMISH template	AF517552.1
foxY	TGCACTGCACTGACTCTGC	CTTTCCATTCCGTGGTGAAG	QPCR	AF517552.1
gataC	GCTGGAGTAGCAAGCAGTCAAG	TGTTACCCATTACCCCAGGATG	WMISH template	NM_214539.1
gataE	TCTTACCCATCAGCCAGGAC	TCGAGTGGAACAATGGAACA	WMISH template	NM_001005725.1
hmg1	GGACCGAGACAGTTCAAAGC	CTTCTCCTCCAGAGCCTTCC	QPCR	SPU_027981
lefty	GAACTTCATACGACAAACATCTCCTGGC	TTTCGATTATATCATATTATTGCATTTTATTATG	WMISH template	SPU_009911
nanos	GCAAGAACAACGGAGAGAGC	CCGCATAATGGACAGGTGTA	QPCR	DQ286228.1
nodal	CACAAAGTGTGTTTGTGCAAG	GTCGATGAAATTGAAAATATCATGA	WMISH template	NM_001098449.1
not	ACGATTTGGAGGGTTTTAAGC	GCAACTTACCCGTCATCACC	WMISH template	NM_214562.1
pax6	GACAGTGTTCTCATCGTGGTG	ACCTCGCGAGAGAAAATCAA	WMISH template	SPU_006786
pitx2	ATCCCAAATTTCCCGTCTTC	TTGGTGGTGTCTCATGTGGT	WMISH template	SPU_004559
scratchX	CGGCCTAACAAGGAGAAAGC	ACGGTTTAATGGTGGAGTGC	WMISH template	SPU_15640
six1/2	TGAAACACCGTCAAAACAAGG	AACTTGTGTCGTGGTCAGTCC	WMISH template	SPU_017379
soxE	GGAGTAGCCCAAGAACACCA	TGACTGTACCTGCGAAGGAG	WMISH template	SPU_016881
ubq	CACAGGCAAGACCATCACAC	GAGAGAGTGCGACCATCCTC	QPCR	SPU_021496